# Structure and intermicellar interactions in block polyelectrolyte assemblies

**Mark Crichton and Surita Bhatia***

*University of Massachusetts, Amherst, USA. E-mail: sbhatia@ecs.umass.edu*

Amphiphilic diblock polyelectrolytes are becoming popular in industrial applications due to their versatility, ranging from usage in pharmaceuticals to personal care products. Many of these systems also exhibit interesting rheological and morphological behavior. Our system is based on a polystyrene-poly(ethyl acrylate) diblock. The properties can be tuned by utilizing a simple hydrolysis reaction, converting poly(ethyl acrylate) (PEA) to poly(acrylic acid) (PAA). We study the effect of this hydrolysis reaction on the interaction between micelles of polystyrene-poly(acrylic acid) in water using small-angle and ultra-small-angle neutron scattering. We see that as more PEA is converted to PAA, the aggregation number and polystyrene core size decrease. We also studied the effect of cationic (DTAB) and anionic surfactant (SDS) on the PS-PAA diblocks using small-angle neutron scattering. We see that as SDS is added, there are no significant changes in the micellar structure. However, on the addition of DTAB past the CMC, we observe changes in the spectra that may correspond to complexation between the PS-PAA micelles and DTAB aggregates.

**Keywords:** **polyelectrolyte; diblock polymer; SANS; USANS**

### 1. Introduction

Amphiphilic diblock polyelectrolytes, consisting of a hydrophobic block and a charged hydrophilic block, are seeing increasing popularity in industrial applications, ranging from usage in personal care products to biomedical and pharmaceutical applications. Such diblocks also show interesting morphological behaviour, as shown by the work of Eisenberg and others (Zhang & Eisenberg, 1995; Cameron *et al.*, 1999).

Our focus has been towards diblock polyelectrolyte gels that have "tunable" rheological properties. Our systems are based on polystyrene-poly(ethyl acrylate) block copolymers, which we hydrolyze to obtain polystyrene-poly(acrylic acid) (Bhatia & Mourchid, 2002). By varying the reaction stoichiometry, we can control the extent of the hydrolysis reaction. Previous work has shown that the elastic modulus and viscosity are strong functions of the extent of the hydrolysis reaction (Bhatia *et al.*, 2001). In addition, the elastic modulus decreases sharply with added anionic surfactant (Bhatia *et al.*, 2001).

In aqueous solution, our copolymers form spherical micelles (Bhatia & Mourchid, 2002). We envision that the unhydrolyzed ethyl acrylate groups, which are hydrophobic, cause an attractive interaction between micelles (Fig. 1). However, the connection between the extent of hydrolysis, micellar structure, and solution rheology is still not well understood. Therefore, small-angle neutron scattering (SANS) and ultra-small-angle neutron scattering (USANS) studies were performed to elucidate the structure of both dilute and concentrated micellar solutions. In addition, the effect of added cationic and anionic surfactant was explored using SANS.

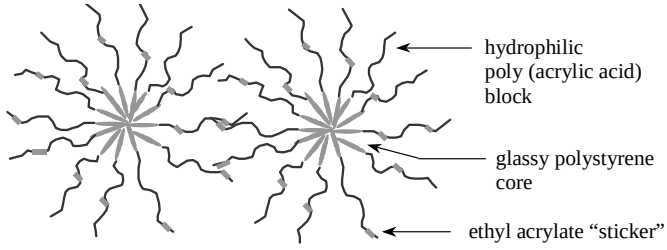


**Figure 1**

Schematic of polystyrene-poly(acrylic acid) micelles, with unhydrolyzed ethyl acrylate groups causing intermicellar association.

### 2. Experimental

The diblock polymers was supplied by Rhodia Inc. as polystyrene-poly(ethyl acrylate). Two different molecular weights were examined, 2000/19468 g/mol and 5300/8100 g/mol (listed as MW of PS block/MW of poly(ethyl acrylate) block). The polymer was supplied as an aqueous suspension of latex particles of approximately 40 wt.%. The hydrolysis reaction was run with 10 wt.% polymer in water at 363 K. When the polymer solution reached 363 K, a 2M NaOH aqueous solution was added dropwise. The amount of NaOH added was dependent on the desired degree of hydrolysis. The reaction mixture was then held at 363 K for 24 h. The final degree of hydrolysis was determined using a 200 MHz $^1$H NMR instrument. After hydrolysis, the polymer was dialyzed using regenerated cellulose membranes with a molecular weight cutoff of 6000-8000 (SpectraPor 1, Spectrum Laboratories) against an aqueous NaOH solution at pH 10 for about one week. This was done to remove impurities and normalize the charge density along the polymer backbone.

Samples for SANS and USANS were prepared by dissolving freeze-dried polymer in $D_2O$ (Cambridge Isotope Labratories) and stirring for several days at 353 K. Calculated scattering length densities, $\rho$, for all relevant molecules are listed in Table 1. Small angle neutron scattering (SANS) measurements were performed on the 30-meter SANS line (NG3) at the NIST Center for Neutron Research (NCNR) in Gaithersburg, MD. Spectra were obtained at 25°C for a polymer concentration of 4.0 wt.%. Quartz sample cells with a path length of 1 mm were used. The detector distances used in these experiments were 1.33 m, 4 m, and 13.1 m, depending on the sample concentration and contrast. Deuterated water was used to quantify the solvent scattering, which was subsequently subtracted from the spectra. Incoherent scattering was estimated from the signal at high $q$ and was also subtracted from the data. The $q$-range covered in these experiments was $0.005\ \text{Å}^{-1} < q < 0.7\ \text{Å}^{-1}$ (where $q = 4\pi \sin\theta/\lambda$ with $\theta$ = half the scattering angle and $\lambda$ = wavelength of the incident neutrons). USANS experiments were performed on NCNR's perfect crystal SANS instrument (BT5). Sample preparation was identical to the SANS samples. Quartz sample cells with a thickness of 1 mm were used.

For the surfactant studies, either dodecyltrimethylammonium bromide (DTAB) from Sigma or sodium dodecyl sulfate (SDS) from Fluka was added to 4 wt.% solutions of the smaller molecular weight diblock (5300/8100) in $D_2O$. The concentrations of DTAB used were 0.2, 0.4, 0.5, 0.6, and 0.8 wt.%, and for SDS the concentrations used were 0.2, 0.3, 0.4, 0.5, 0.6 wt.%.

  

**Table 1**

Scattering length densities, $\rho$, of relevant molecules.

| Species | $\rho$ ($10^{-6}$ Å$^{-2}$) |
|---|---|
| poly(ethyl acrylate) | 0.8446 |
| polystyrene | 1.21855 |
| $D_2O$ | 6.37225 |
| poly(sodium acetate) | 4.2698 |

### 3. Results and discussion

#### 3.1. SANS on varied extent of hydrolysis

Samples of the larger molecular weight diblock (2000/19468) were hydrolyzed to different degrees as discussed in section three. The extent of hydrolysis is described by the value *f*, which can vary between zero and one. A *f* value of zero is the case where none of the poly(ethyl acrylate) is hydrolyzed, and a *f* value of one is the case where the poly(ethyl acrylate) is completely converted to poly(acrylic acid).

The SANS data were modelled by using a polydisperse spherical form factor:

$$F(q)=\int_0^\infty \frac{9}{\sqrt{2\pi}\sigma} e^{-\frac{(r-R_{\rm core})^2}{2\sigma^2}} \frac{(\sin(qr)-qr\cos(qr))^2}{(qr)^6} dr \tag{1}$$

This two-parameter form factor includes $R_{\rm core}$, the average sphere radius, and $\sigma$, the standard deviation of the sphere size distribution. We interpret $R_{\rm core}$ and $\sigma$ as characteristic of the polystyrene core size distribution.

For the structure factor, we utilized the adhesive hard sphere model as defined by Baxter (1968), which includes the hard-sphere radius $R_{\rm interaction}$, a dimensionless temperature $\tau$ which describes the micellar attractions, and the volume fraction of spheres, $\phi$, as fitting parameters. To incorporate polydispersity effects into the structure factor, we use the method of Kotlarchyk and co-workers (1984), who define a polydispersity correction factor $\zeta$ as:

$$S'(q)=1+\zeta(q)\left[S(q)-1\right] \tag{2}$$

$$\zeta(q)=\frac{\left|\int_0^\infty \frac{3}{\sqrt{2\pi}\sigma} e^{-\frac{(R-R_{\rm ave})^2}{2\sigma^2}} \frac{(\sin(qR)-qR\cos(qR))}{(qR)^3} dR\right|^2}{\int_0^\infty \frac{9}{\sqrt{2\pi}\sigma} e^{-\frac{(R-R_{\rm ave})^2}{2\sigma^2}} \left|\frac{(\sin(qR)-qR\cos(qR))}{(qR)^3}\right|^2 dR} \tag{3}$$

The scattered intensity is then expressed as:

$$I(q)=N(\Delta\rho)^2 F(q)S'(q) \tag{4}$$

To reduce the number of fitted parameters, we must recognize that parameters $\phi$ and $R_{\rm interaction}$ are not independent; they are related through the number density of scatterers *N*:

$$\phi=\frac{4\pi}{3}R_{\rm interaction}^3 N \tag{5}$$

For our system, *N* represents the number density of micelles, which can be calculated as:

$$N=\frac{cN_{\rm AV}}{MW_{\rm PS\text{-}PAA/EA}N_{\rm agg}} \tag{6}$$

where *c* is the concentration of the polymer in solution, $MW_{\rm PS\text{-}PAA/EA}$ is the molecular weight of the polymer, $N_{\rm AV}$ is Avogadro's number, and $N_{\rm agg}$ is the aggregation number, defined as:

$$N_{\rm agg}=\frac{4\pi}{3}\frac{R_{\rm core}^3}{V_{\rm PS}} \tag{7}$$

Here, $V_{\rm PS}$ is the volume of the polystyrene block (3666 Å$^3$). Combining equations (5), (6), and (7) leads to the following expression for $\phi$:

$$\phi=\left(\frac{R_{\rm interaction}}{R_{\rm core}}\right)^3 \frac{cMW_{\rm PS}}{\rho_{\rm PS}MW_{\rm PS\text{-}PAA/EA}} \tag{8}$$

where $\rho_{\rm PS}$ is the mass density of polystyrene, and $MW_{\rm PS}$ is the molecular weight of the polystyrene block. Fitting the data using the adhesive hard sphere structure factor and polydisperse form factor thus requires four parameters: $\sigma$, $R_{\rm core}$, $R_{\rm interaction}$, and $\tau$.

All of the 4.0 wt.% polymer solutions formed strong gels. Fig. 2 shows the experimental data from the 30-meter instrument (NG3) at the NIST Center for Neutron Research. A strong peak is observed at ~0.01 Å$^{-1}$ for all the samples, which we believe corresponds to the intermicellar distance in these gels. The observed peak gets sharper and more intense as *f* decreases. By contrast, the peak position remains fairly constant with *f*, varying from 0.0102 Å$^{-1}$ to 0.0113 Å$^{-1}$ for this series of data. The results from our fits to the data are given in Table 2. The aggregation number was calculated using equation (6).

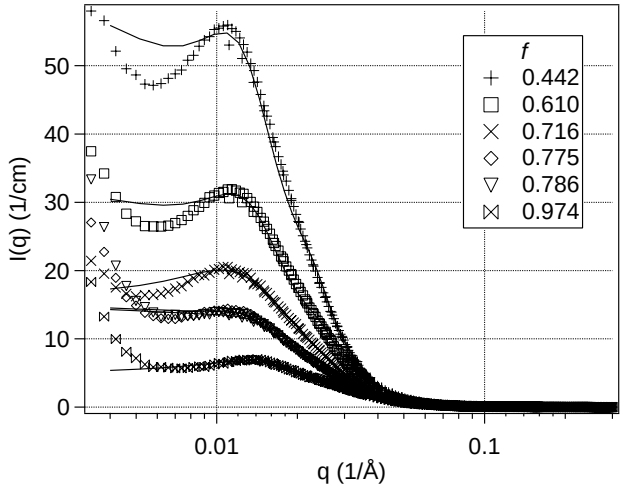


**Figure 2**

30-meter SANS results from 4 wt.% PS-PAA gels in $D_2O$.

We found that micelle core radius, and hence the aggregation number, decrease as *f* increases (Table 2). There are two possible explanations for this trend. First, the effective size of the corona chains could increase as *f* increases due to the increasing charge density. Thus, a smaller number of chains would be able to be packed into each micelle, resulting in a decrease in $N_{\rm agg}$. The other

explanation is that the unhydrolyzed ethyl acrylate groups are concentrated near the polystyrene core. As seen in Table 1, the scattering length density difference between PEA and $D_2O$ is similar to the difference between PS and $D_2O$, which would result in an apparent increase in the core size.

**Table 2**

Results from structure factor/form factor fitting of 30-meter SANS data on 4 wt.% gels in $D_2O$.

| $f$ | MW Polymer | $R_{core}$ (Å) | $N_{agg}$ | $\tau$ | $\sigma$ (Å) |
|---|---|---|---|---|---|
| 0.442 | 18970 | 106.6 ± 0.1 | 1385.8 | 0.073 ± 0.001 | 26.481 ± 0.028 |
| 0.610 | 18020 | 98.9 ± 0.1 | 1104.6 | 0.069 ± 0.001 | 24.513 ± 0.292 |
| 0.656 | 17760 | 100.4 ± 0.1 | 1155.0 | 0.009 ± 0.003 | 27.919 ± 0.046 |
| 0.716 | 17421 | 96.2 ± 0.7 | 1016.7 | 0.034 ± 0.002 | 25.705 ± 0.036 |
| 0.786 | 15926 | 95.0 ± 0.1 | 980.3 | 0.042 ± 0.001 | 26.213 ± 0.042 |
| 0.974 | 15926 | 76.1 ± 0.1 | 503.1 | 0.000 ± 0.013 | 20.388 ± 0.042 |

As can be seen in Table 2, the uncertainty in the fitted parameters is quite low, other than the stickiness parameter, $\tau$. This may be due to the large experimental error present at low $q$, which is the range that is most sensitive to the value of $\tau$. It is worth mentioning that while the adhesive hard sphere model fails to yield a good interaction parameter, it appears that some form of an attractive component is needed to successfully fit the data. An attempt to model the data using a hard sphere structure factor yielded unphysical results (e.g., unrealistic values for the micellar volume fraction).

To gain insight into the origin of the low $q$ scattering, USANS was also performed on the asymmetric polymer diblocks. The results are shown in Fig. 3. The USANS data shown was desmeared utilizing a minimization procedure developed at NIST. The data exhibit power-law behaviour over approximately two decades in $q$. The $q$-range over which the USANS data are taken corresponds to probing length scales of roughly 1000 - 20,000 Å (100 nm - 2 µm); note that the upper limit is much larger than the size of a single micelle. Thus, we believe that this power-law scaling is indicative of a large length scale structure in solution; i.e., formation of micellar aggregates and perhaps an associated network of micelles.

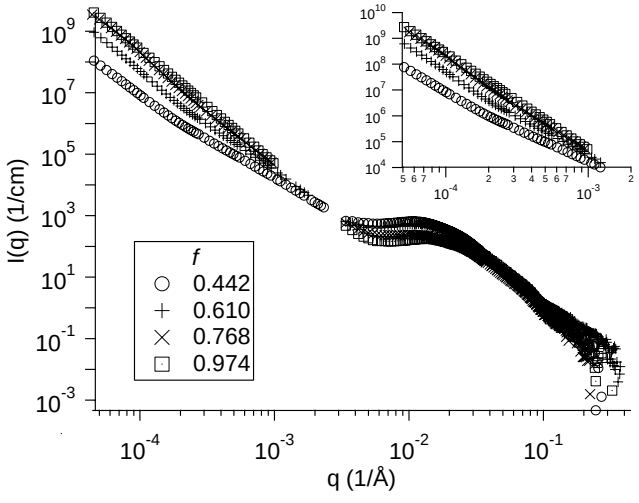


**Figure 3**

USANS and SANS results for 4 wt.% gels in $D_2O$. Inset is a magnified view of the USANS data.

The desmeared data was fit with a power law, $I(q) \sim q^d$, and Table 3 summarizes the USANS data fits. We observe a change of the exponent $d$ from -2.82 to -3.69 as $f$ increases. Oftentimes, the value of this exponent in the low $q$ regime is interpreted as a fractal dimension, particularly for attractive colloidal spheres that form fractal flocs, where values of -1.7 to -2.2 have been reported. However, if this were the case, we would expect a value of $d$ between -1 and -3. Values in the range of -3 to -4, as we observe, may indicate surface scattering from large objects or aggregates. In this case, the exponent would characterize the aggregate interface. The trend in $d$ is consistent with our physical picture of ethyl acrylate "stickers" and intermicellar attraction. For lower values of $f$, there is a significant number of ethyl acrylate "stickers" present. We envision that this leads to an attractive force and formation of large micellar aggregates, which may have a loose, open structure and ill-defined interface. Thus, we believe that the exponents that we extract from this data are characteristic of the interface between micellar aggregates and the surroundings.

**Table 3**

Values of the slope from a power law fit of the USANS data.

| $f$ | $d$, power-law exponent |
|---|---|
| 0.442 | -2.82 |
| 0.610 | -3.37 |
| 0.786 | -3.72 |
| 0.974 | -3.69 |

### 3.2. Addition of surfactant

Cationic (DTAB) and anionic (SDS) surfactants were added to the symmetric diblock polymers with $f = 0.85$. The scattering results for SDS are shown in Fig. 4. As mentioned above, previous work (Bhatia *et al.*, 2001) has shown that the rheology of the system transitions from a gel to a liquid as SDS is added. However, our SANS spectra show almost no change with addition of SDS, other than a decrease at low $q$. The main peak in the spectra does not disappear or shift as the amount of SDS increases. Thus, the micellar structure is preserved upon addition of SDS, and the intermicellar spacing does not change appreciably. The change at low $q$ may be indicative of a disruption of the large length scale structure and reduced intermicellar attractions due to the screening of the hydrophobic groups by SDS.

Addition of DTAB is also known to significantly affect the rheology, first causing an increase in the elastic modulus, followed by a decrease (Heitz & Joanicot, 2001; Crichton & Bhatia, 2002). Fig. 5 shows the spectra that result on addition of DTAB to the system. Here, we see a dramatic shift of the main peak to higher values of $q$; the peak position varies from 0.0126 $Å^{-1}$ to 0.0158 $Å^{-1}$ over this data series. As the amount of DTAB increases, the peak shifts to higher $q$ and slowly broadens. Note that the concentrations of DTAB used are, in some cases, above the CMC of 4.56 g/l, which roughly corresponds to 0.5 wt.% of DTAB. However, the size of a DTAB micelle is roughly 40 Å in diameter, which corresponds to a $q$ value of about 0.6 $Å^{-1}$ (Tavernier *et. al.*, 1998). There is no formation of a peak in that $q$ range, so it can be assumed that instead of single DTAB micelles forming, there is some PS-PAA/DTAB complex formation. This could decrease the intermicellar spacing, which is consistent with the peak shift that we observe. This behaviour could also be caused by the DTAB causing the shrinkage of the negatively charged PAA corona.

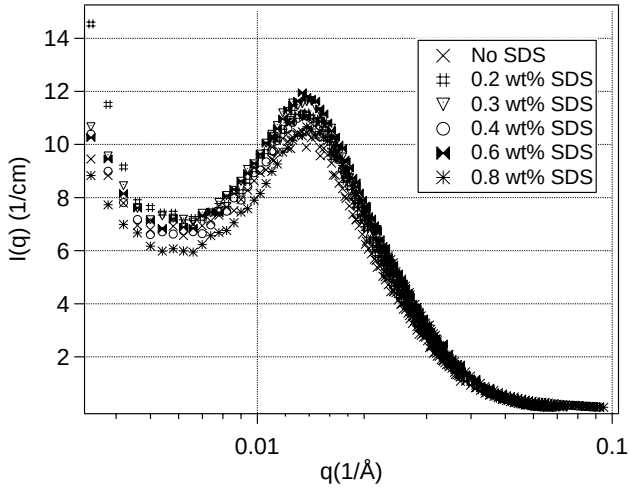


**Figure 4**

30-meter SANS results for 4 wt.% symmetric PS-PAA in $D_2O$ with added SDS.

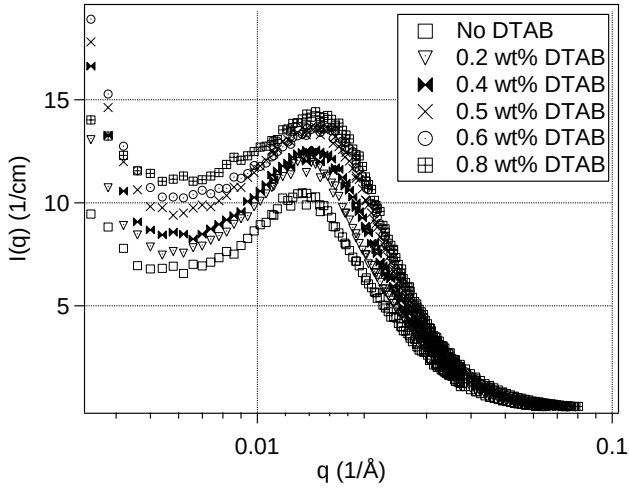


**Figure 5**

30-meter SANS results for 4 wt.% symmetric PS-PAA in $D_2O$ with DTAB added.

## 4. Conclusions

### 4.1. Effect of hydrolysis reaction

We observe a decrease in the micelle aggregation number, $N_{agg}$, as the extent of hydrolysis $f$ increases. We believe that there are two possible explanations for this trend. First, as $f$ increases, the corona has a higher charge density as more of the neutral ethyl acrylate groups are converted to acrylic acid groups. This in turn causes chains to be excluded from the micelle due to the strong electrostatic repulsion between the poly(acrylic acid) chains, which decreases the aggregation number. Second, due to the nature of the hydrolysis reaction, we could have the case where the outside layer of the micelle is converted easily to poly(acrylic acid). However, closer to the core, the hydrolysis reaction might not be as complete due to steric interactions. This in turn leads to a larger concentration of ethyl acrylate near the polystyrene core, which leads to a larger apparent core size and aggregation number. The stickiness parameter $\tau$ shows no clear trend in $f$. This suggests that the adhesive hard sphere model might not be a suitable model to describe the micelle-micelle interactions of the system. Furthermore, it was observed that the fits of the experimental data using the adhesive hard sphere model did not handle the increase at low $q$. Our USANS data suggests that the low q scattering may be due to formation of aggregates of micelles or other large strctures, which would not be captured by the adhesive hard sphere model.

### 4.2. Effect of surfactant

From our SANS studies, it is clear that there is no change in the main peak upon addition of SDS, in spite of the dramatic change in the rheology that has been reported (Bhatia *et al.*, 2001). This suggests that as SDS is added to the system, the structure of the micelles is not changed. However, SDS molecules might be screening the micelle-micelle interactions, which is consistent with the observed rheology. We propose that the hydrophobic tail of SDS is screening the hydrophobic ethyl acrylate groups in the corona. This will weaken the ethyl acrylate interactions between micelles, leading to weaker attractions. After enough SDS is added to the system, the ethyl acrylate attractions can no longer hold the micellar gel together, resulting in a fluid with low elasticity.

On addition of DTAB, a cationic surfactant, something radically different occurs. A shift and broadening of the main peak is seen in the SANS data. From rheology, we observe that $G'$ increases up to about 0.4 wt.% DTAB, then rapidly falls of at 0.6 wt.% DTAB (Crichton & Bhatia, 2002). The peak shift occurs at about 0.4 wt.% DTAB. There are two possible explanations for this peak shift. First, as we approach the CMC of DTAB, there could be the formation of DTAB and PS-PAA complexes, which change the morphology of the micelle and intermicellar distance drastically. Second, with the addition of this cationic surfactant, the negatively charged corona could collapse, leading to a smaller micelle. Finally, a combination of these two effects cannot be ruled out.

We acknowledge B. Hammouda, S. Kline, and J. Barker at the NIST Center for Neutron Research in Gaithersburg for their vast assistance in performing these experiments and the support of the National Institute of Standards and Technology, U. S. Department of Commerce, in providing the neutron facilities used for portions of this work. Our data is partially based upon activities supported by the National Science Foundation under Agreement No. DMR-9986442. The Rhodia Complex Fluids Laboratory provided us with the polystyrene-poly(ethyl acrylate) diblocks, and we particularly thank A. Mourchid, M. Joanicot, G. Lizzaraga, and D. Bendejacq of Rhodia. Finally, we would like to acknoweldge financial support from the Rhodia Complex Fluids Laboratory and a University of Massachusetts Faculty Research Grant.

**References**

Baxter, R. J. (1968). *J. Chem. Phys.* **49**, 2770-2774.
Bhatia, S. R. & Mourchid, A. (2002). *Langmuir.* **17**, 6469-6472.
Bhatia, S. R., Mourchid, A. & Joanicot, M. (2001). *Curr. Opin. Colloid Interface Sci.* **6**, 471-478.
Cameron, N. S., Corbierre, Muriel K. & Eisenberg, A. (1999). *Can. J. Chem.* **77**, 1311-1326.
Crichton, M. A. & Bhatia, S. R. (2002). In preparation.
Kotlarchyk, M., Chen, S. H., Huang, J. S. & Kim, M. W. (1984). *Phys. Rev. A.* **29,** 2054-2069.
Heitz, C. & Joanicot, M. (2001). Unpublished data, Rhodia Complex Fluids Laboratory.
Tavernier, H. L., Barzykin A. V., Tachiya, M. & Fayer, M. D. (1998). *J. Phys. Chem.* **102**, 6078-6088.
Zhang, L. F. & Eisenberg, A. (1995). *Science.* **268**, 1728-1731.

 Received 29 August 2002 • Accepted 17 March 2003 